Acta Crystallographica Section D
Biological Crystallography
ISSN 0907-4449

A new rotation function for molecular replacement by using both the self and cross Patterson vectors

Fan Jiang

Beijing National Laboratory for Condensed Matter Physics, Institute of Physics, Chinese Academy of Sciences, Beijing 100080, People's Republic of China

Correspondence e-mail: fjiang@aphy.iphy.ac.cn

Received 15 January 2008
Accepted 4 March 2008

The rotation function in molecular replacement is traditionally computed in reciprocal space. The common practice is to use a Patterson vector radius of about the size of the target molecule to limit the interatomic vectors to match only the Patterson self-vectors. In real space, the molecular image of a search model can be searched and matched to the Patterson function vector space. Depending on which asymmetric unit the matched Patterson vectors are in, both self or cross Patterson vectors can be matched to the search model. The algorithm described here for computing the rotation function is to average the signals from all images found by the image-seeking functions in the Patterson vector search. Tests show that a search model consisting of a two-helix fragment can be found in a myoglobin crystal using experimental data in a global rotation search. This demonstrates that the new rotation function is a potentially useful approach.

1. Introduction

Molecular replacement is one of the most widely used phasing methods for structure determination in protein crystallography (Blow, 2006; Brünger *et al.*, 1987; Brünger, 1997; Huber, 1965; Navaza, 1987; Rossmann & Blow, 1962; Machin, 1985; Dodson *et al.*, 1992; Carter & Sweet, 1997). As structural genomics progresses rapidly and more novel structures are being determined, the molecular-replacement method has become the new focus of many developments (Bricogne, 1997; Read, 2001; Storoni *et al.*, 2004; Vagin & Teplyakov, 1997). The phase information obtained from molecular-replacement solutions can sometimes be modified and combined with phases obtained using other methods (Morris *et al.*, 2002; Read, 2006; Terwilliger, 2000; Zhang *et al.*, 2006) to generate traceable maps. This offers the opportunity of using molecular replacement as a potential method for *ab initio* phasing.

As the molecular-replacement method is based on the maximum overlap between the self-vectors of the Patterson function of the target molecule and the search model (Rossmann & Blow, 1962), the method can also be visualized in real space as an image-seeking problem in Patterson vector space (Buerger, 1959). If the interatomic vectors in the search model are the signals to be detected and those in the target molecule are the background noise, then as the size of the target molecule increases relative to the search model the level of background noise of the Patterson function (the interatomic vectors) will approach the signal level. Furthermore, the peaks in the Patterson function may not correspond to the atom positions in the model. Moreover, it is often the case that only a small fragment of the target molecule is known. Thus, it is

generally difficult to detect the signal of the search model in order to determine its orientation.

With recent increases in available computing power, it is possible to conduct a six-dimensional search that will simultaneously find the orientation and the position of a search model (Chang & Lewis, 1997; Kissinger *et al.*, 1999; Glykos & Kokkinidis, 2000; Liu *et al.*, 2003). This approach has enabled higher signal-to-noise ratios for smaller search models. Jiang & Rao (2001) also implemented a six-dimensional search method but in real Patterson space by searching the rotations exhaustively and then searching the translations with a fast vector-matching algorithm (Jiang & Kim, 1991). The six-dimensional searches have the ability to utilize both the self and cross Patterson vectors in calculating the overlap between the search model and the experimental Patterson map. This ability is believed to be the primary reason why smaller models can be searched and higher signal-to-noise ratios can be obtained.

The real-space implementation of rotation functions (Hoppe & Paulus, 1967; Nordman & Nakatsu, 1963; Nordman, 1966, 1972, 1994; Schilling, 1970) is essentially equivalent to the reciprocal-space implementation and has been shown to work for single-helix models for rotation searches in a myoglobin crystal (Nordman, 1972, 1994). However, in these rotation searches only the self-Patterson vectors are included in the matching with the model vectors.

Other rotation functions have been developed to enhance the reliability and signal-to-noise level of the molecular-replacement method. The direct rotation-search method is based on Patterson correlation search and refinement (Brünger, 1997). The maximum-likelihood method is based on Bayesian statistics and fast Fourier transform (Read, 2001; Storoni *et al.*, 2004).

Here, a novel method of computing the rotation function in real space is described. Because the overlaps of different Patterson vectors at different locations in a unit cell are different, the background-noise matches resulting from the matches between the model vectors and the experimental Patterson vectors will be different. In contrast, the true matches will be similar and persistent everywhere. By averaging the signals from all the matches at different locations, we expect that the signals of the true matches will be increased greatly. The method is tested by performing a global search for a two-helix fragment in a myoglobin crystal. It is shown that our method is able to find the expected rotation-function peaks in the test.

2. Materials and methods

2.1. The method of matching both the self and cross Patterson vectors

$$\mathbf{y}_i' = R\mathbf{y}_i + \mathbf{t}, \tag{1}$$

$$\mathbf{y}_i'' = S_1\mathbf{y}_i' + \mathbf{t}_1, \tag{2}$$

$$\mathbf{v}_\mathrm{p} = \mathbf{x}_i'' - \mathbf{x}_j \cong \mathbf{u}_\mathrm{p} = \mathbf{y}_i'' - \mathbf{y}_j = S_1R\mathbf{y}_i + S_1\mathbf{t} + \mathbf{t}_1 - \mathbf{y}_j, \tag{3}$$

$$\mathbf{v}_\mathrm{p} \cong S_1R\mathbf{y}_i + \mathbf{u}_{t,j}. \tag{4}$$

The convention used for the variable names is as follows: '**x**' is for real atomic coordinates, '**y**' for coordinates from the model, '**v**' for vectors from the real Patterson and '**u**' for vectors computed from the model. In the above equations, $\mathbf{x}_i$ and $\mathbf{y}_j$ are the atoms in the target molecule and the search model, respectively, and $\mathbf{v}_\mathrm{p}$ are the target Patterson vectors. (R, $\mathbf{t}$) is a rigid-body transformation. (S_1, $\mathbf{t}_1$) is a symmetry operation. In (3), it is assumed that the model atom $\mathbf{y}_i''$ has a counterpart atom $\mathbf{x}_i''$ in the target. For any given rotation R, the first term on the far right side of (3) is known. Since for any given crystal $\mathbf{v}_\mathrm{p}$ is also known, the only undetermined variables are the translation vector $\mathbf{t}$ and the target atom $\mathbf{x}_j$; here, the counterpart atom $\mathbf{x}_j$ has been substituted for the model atom $\mathbf{y}_j$. This statement is further simplified by (4), where $\mathbf{u}_{t,j}$ is an unknown vector. Given the matches between the vectors $\mathbf{v}_\mathrm{p}$ and the vectors in the first term on the far right side of (4), many vectors of $\mathbf{u}_{t,j}$ are possible. For any given match between the search model and the target, the vector $\mathbf{t}$ in (1) is in fact determined and the real variable is the target atom $\mathbf{x}_j$. Therefore, for every target atom $\mathbf{x}_j$ there are a set of vectors from the search model that can potentially be matched to the target Patterson vectors $\mathbf{v}_\mathrm{p}$.

In other words, according to Buerger (1959), (4) is in fact searching for the model image in the Patterson function vector space. To explicitly name the point atom of the vector set of an image, it is called the 'pivotal' atom here. Furthermore, the atoms in the image are called 'vector' atoms. The vector set in the Buerger convention (Buerger, 1959) contains the vectors from the pivotal atom to the vector atoms. In (4), these vectors are transformed by a fixed difference vector $\mathbf{u}_{t,j}$. If (S_1, $\mathbf{t}_1$) is an identical symmetry operation, the Patterson vectors matched are self-vectors. If it is any other symmetry operation, the vectors matched are cross-vectors. It is also worthwhile noting that if the pivotal atom is a heavy atom, such as the Fe atom in myoglobin, the associated set of vectors will have a higher weight than those for other pivotal atoms.

Our rotation function is based on the matching equation shown in (4). Firstly, several matching characteristics (image-seeking functions according to Buerger, 1959) of the search model are calculated and averaged over all the target atoms or all the images found in the Patterson function. A signal-processing technique is then used; that is, the averaged characteristics are combined linearly using a set of optimal weights derived from the multiple linear regression method and the combined score is then used as the rotation function.

2.2. Sampling of the rotation space

It is very difficult to sample rotation space uniformly. Lattman has designed an angle convention for sampling Eulerian angles (Lattman, 1972). The advantages of using Eulerian angles are particularly pronounced when a rotation search is conducted in the reciprocal-space implementation of the rotation function with crystallographic symmetries.

However, in this work polar angles are used to sample the rotation space globally. Firstly, the quaternion convention is used to generate the rotation matrix and the polar angles. Since the sum of the four components of a quaternion is unity, the order in which each component is generated can be permutated. For a given order of the four components, each component is generated randomly within the appropriate range. Permutation of the order of the four components ensures further randomization and better uniformity. 10^6 polar angles are generated this way. Then, for any two polar angles their angle distance is calculated. If it is less than 4°, one of the two angles is removed. This removes the redundancy in the sampling and results in approximately 10^5 angles.

2.3. The algorithm for computing the rotation function

The rotation space is sampled exhaustively with polar angles as described above. Vector matching is performed with a translation-search algorithm in real space. The translation-search algorithm is based on a digitized translation-vector space (Jiang & Kim, 1991; Jiang & Rao, 2001). A one-dimensional case of this algorithm is illustrated in Fig. 1, in which a set of vectors in one dimension is matched to another set. The inter-set translation vectors between the first set and the second set are calculated, which are just the difference vectors. The corresponding matching scores are then stored in a translation-vector space, also in one dimension, according to the positions of the difference vectors. In Fig. 1, when the difference translation vector $\mathbf{T}_x = 1$, three vectors are matched between the two sets and a peak is found in the distribution of matching scores in the translation-vector space. In the three-dimensional case, the algorithm works by the same principle. The peaks are searched in the distribution of matching scores in the three-dimensional translation-vector space.

Since the Patterson function vectors are weighted, the matches between the vector sets are also weighted. Three common image-seeking functions are implemented in our method: the product of the weights, the correlation coefficient of the weights and the relative *R* factor of the weights between the Patterson vectors and the model atoms.

2.4. Testing with a myoglobin crystal structure using experimental diffraction data

The new method was tested using a myoglobin crystal structure with deposited experimental data. Both the crystal structure and the diffraction data were downloaded from the Protein Data Bank (PDB; http://www.rcsb.org) with PDB code 1dti. The space group is $P2_12_12_1$, with unit-cell parameters $a = 49.163$, $b = 40.002$, $c = 80.011$ Å and with one molecule in an asymmetric unit. The experimental diffraction data for this entry 1dti were available to 1.7 Å resolution. Another myoglobin crystal structure (PDB code 1a6m) was also used in the tests. Its space group is $P2_1$, with unit-cell parameters $a = 63.800$, $b = 30.810$, $c = 34.350$ Å, $\beta = 105.80°$ and one molecule in an asymmetric unit. The diffraction data for this entry were available to 1.0 Å resolution.

In the tests, the experimental Patterson map was initially calculated using data between 20 and 3.0 Å resolution. Firstly, the diffraction amplitude was normalized (using *ECALC* from *CCP*4; Collaborative Computational Project, Number 4, 1994). The Patterson map was then calculated using the normalized amplitude (using *FFT* from *CCP*4). To make sure that no cross Patterson vectors were missed, the Patterson map was extended to double the unit cell; that is, with a range from 0 to 2.0 along each unit-cell axis (using *EXTENDS* from *CCP*4). The Patterson function vectors were then output by writing out grid points with function values more than 1.0σ (using a modified version of *PEAKMAX* from *CCP*4 called *PEAKMAXGRD*). The output grid points were in PDB coordinate format. This file was manually edited to remove the origin peaks, which were usually the highest peaks and obviously close to the origin. The edited file was then used as input for the experimental Patterson function vectors.

Three matching functions or image-seeking functions (Buerger, 1959) were used in our method. The first function is the product of the weights between the Patterson vectors and the model atoms matched. The second function is the correlation coefficient of the weights between the Patterson vectors and the model atoms matched. The third function is the relative *R* factor between the weights of the Patterson vectors and the model atoms matched. In the translation space, peaks could be searched according to any one of the three functions, corresponding to three peak modes. For any given peak mode, each peak has a peak score and two other scores that could be fetched at the same peak position in the other two score distributions. However, these three scores are not used directly. Instead, they are averaged over all the peaks in the translation-vector space for the given peak mode. It is the average scores that are output for computing the rotation function. This is equivalent to averaging over all the pivotal atoms with good matches or signals. Alternatively, it is equivalent to averaging over all the good images found by the given image-seeking function in the Patterson function. A fourth score is then output which is the average number of model atoms (or digitized grids) that have been matched to the Patterson vectors in calculating the given image-seeking

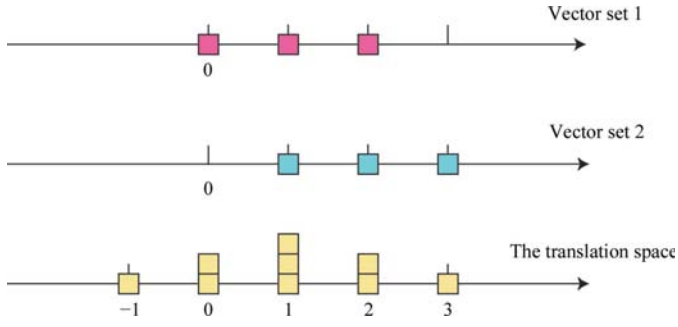

Figure 1
A schematic diagram of the translation-search algorithm in one-dimensional space. The best translation for the simple example shown is one grid step along the *x* axis. The three-dimensional spaces of the search model, the Patterson vectors and the translation vectors are all digitized with the same grid spacing.

Table 1
Rotation-function peaks using a two-helix fragment as the search model.

Solution No.	Rank	φ (°)	ψ (°)	χ (°)	Peak height (σ)
1	11	190.5	111.2	3.2	2.90
2	22	73.8	90.0	7.4	2.79
3	31	0.0	0.0	0.0	2.70
4	71	206.2	59.8	5.3	2.43
5	96	208.8	6.5	9.3	2.29
6	111	195.5	170.7	5.4	2.20

function. Finally, a fifth score is output which is the number of peaks found in the translation space for the given peak mode and used for averaging.

Therefore, the rotation search is usually run three times with three different peak modes. By merging the three sets of five scores from each peak mode, a total of 15 scores will be output for each rotation sampled. A signal-processing technique such as the multiple linear regression method is then used to optimize a set of weights for a given model and a crystal structure and to combine the 15 scores to compute a total score, which is used as the rotation-function value. It is expected that the peaks of this new rotation function should correspond to the correct orientations. This new method has been implemented in real space and tested on a two-helix fragment from residues A3 to A36 of 1dti using the main-chain atoms (N, CA, C and O) only. For the search model, the atomic coordinates were directly used for computation of the image-seeking functions.

3. Results

The purpose of the tests was to demonstrate that the new rotation function could work similarly to other known rotation functions for molecular replacement. A two-helix fragment from myoglobin was used as the search model, as shown in Fig. 2. Diffraction data from PDB entry 1dti were used to calculate the Patterson function. A global rotation search was performed using a grid size of 4 Å. Firstly, a set of normalization factors and relative weights was optimized by performing a local rotation search about the native identical solution in the crystal structure. The resulting correlation between the rotation distance and the optimized rotation function was 0.6030.

A global rotation search was then performed. The rotation function was computed according to the relative weights optimized from the multiple linear regression method and peaks were found and sorted. Table 1 lists the rotation-function solutions whose rotation-angle distances are less than 10° from the identical rotation. It can be seen that there are five correct solutions in the top 100 candidate solutions, including the identical solution, which is ranked as the 31st solution. Table 1 also shows that the peak heights of the correct solutions are above 2σ. These results show that the new rotation function works reasonably well in the current test.

To test the generality of the relative weights, another myoglobin crystal structure (PDB code 1a6m) was used.

Table 2
Optimized relative weights for the computation of the rotation function.

The native set was obtained by including only crystal structure 1dti in the training set. The merged set was obtained by including 1dti, 1a6m and several artificial crystal structures. The search model was either residues A3–A36 of 1dti or the same fragment from 1a6m superimposed on 1dti.

Score notation	Native set	Merged set
FP-1	−1.114731	−5.871909
Corr-1	−0.043121	0.133801
Npair-1	0.063635	0.414468
Rfac-1	0.352831	−3.920085
Navg-1	−0.199072	0.151711
FP-2	1.086858	5.840462
Corr-2	−0.283821	−0.690696
Npair-2	−0.411570	−0.579139
Rfac-2	0.282967	−0.908377
Navg-2	0.156114	−0.067345
FP-3	0.614148	0.427881
Corr-3	−0.263527	−0.416576
Npair-3	−0.069208	−0.119076
Rfac-3	−0.036298	3.577076
Navg-3	0.003657	−0.113181

Before optimizing the weights, the 15 scores were first normalized by converting them to Z scores. It is clear that the relative weights would be affected by the range of scores included in the training set. However, in our case the relative weights seemed to be more dependent on a specific model, whereas the normalization factors (average and standard deviation) seemed to be more dependent on the crystal structures included in the training set. Although this observation was not conclusive, a combination of one set of weights and another set of normalization factors obtained separately worked in at least one test case. When several crystal structures, including true crystal structures with different space groups and artificial structures with box-shaped unit cells, were merged into one training set to obtain a merged set of normalization factors and weights, the merged set seemed much more general (see Table 2). When this set was applied to the global search test shown above, there were 13 correct orientations in the top 200 candidate solutions. They were ranked at 34, 46, 71, 74, 75, 76, 89, 116, 119, 121, 138, 189 and 196. The identity rotation (0, 0, 0) was ranked at 75. Both the native set and merged set of weights are shown in Table 2.

To see whether it was necessary to use all 15 scores for the computation of the rotation function, the correlation coeffi-

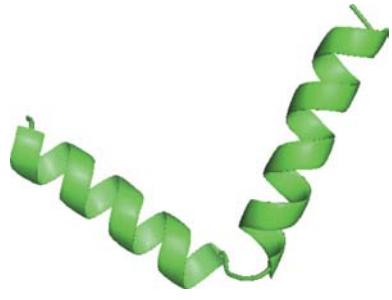

Figure 2
The two-helix search model used in the global rotation search. It consists of the main-chain atoms of residues A3–A36 of the myoglobin structure 1dti. The main-chain atoms include the N, CA, C and O atoms.

cients between the angle distance and each score were checked. The highest correlation coefficient was achieved by the correlation coefficient score in peak mode 2, with a value of 0.2439. The product score was the second highest, with a value of 0.2106. These results are consistent with what is observed in other rotation functions. Therefore, it is possible to use only one type of score to compute the rotation function, especially in the reciprocal-space implementation (see §4). For the real-space implementation, it is better and more robust to use the combined score from the 15 scores.

To see the effect of including the cross-vectors in the Patterson search, the self-vectors were extracted from the Patterson map by applying a radius cutoff of 15 Å around the origin. The same global search was then performed. Using weights optimized for the self-vectors, which produced a correlation coefficient of 0.4923 for the angle distance, the rotation-function values were calculated. The first correct orientation was ranked at 205, with a rotation of (86.28, 50.65, 5.488°). This result is consistent with the lower correlation coefficient obtained from weight optimization using only the self-vectors.

4. Discussion

The proposed rotation function is the first method that utilizes both the self and the cross Patterson vectors in computing the rotation function in molecular replacement. The traditional method of computing the rotation function is to integrate the Patterson correlation within a volume around the origin by limiting the length of the interatomic vectors so that the majority of the integration arises from the self Patterson vectors. By interpreting the Patterson vector equation (4) in a novel way based on the image-seeking method (Buerger, 1959) in Patterson vector space, the technique of averaging over the signals (or the images) is used to reduce the noise from the background matching. As a result, a new rotation function is defined. In this novel interpretation, the 'pivotal' atoms represent those atoms in the target molecule that lead to genuinely good matches with the search model, while the 'vector' atoms correspond to the atoms in the search model matched to the counterpart image atoms in the target molecule. Thus, there is some similarity between our method and Buerger's image-seeking method. The difference is that our method further makes use of averaging to enhance the signals from the many model images found in the Patterson function vector space. Because of the overlap of the vectors in the Patterson function, there are many false-positive matches in the image-seeking functions. However, these false-positive background-noise matches tend to average out. Indeed, our results show that for the search model tested, this approach seems to be valid. Therefore, in the real-space implementation the new rotation function for molecular replacement can utilize the signals from both the self and the cross Patterson vectors in a way that has not previously been possible.

It should be pointed out that our method could also be implemented in reciprocal space. Using (4), it is clear that the Patterson vectors are matched with the model vectors, instead of the interatomic vectors of the model. The matching between the two sets of vectors is equivalent to constructing a translation function and finding the translation peaks at difference vector $\mathbf{v}_r$. The reciprocal implementations of similar translation functions using a fast Fourier transform has been used for shape matching in molecular docking (Chen *et al.*, 2003; Katchalski-Katzir *et al.*, 1992) and in crystallography. In fact, the reciprocal implementation of (4) may also be considered as a variant of the phased translation function (Bentley, 1997; Colman & Fehlhammer, 1976; Vagin & Teplyakov, 2000). For example, the product score of the new rotation function can be computed by first performing a Fourier transform with coefficients $F_c \exp(i\varphi_c) F_o^2$. Searching for the peaks in the translation map and averaging the peak heights then gives the product score for the new rotation function. The reciprocal implementation will in general have higher computation efficiency. For the current real-space implementation, the global search performed for the two-helix model took about 30 h of CPU time (3.0 GHz) using a grid size of 4 Å for the translation-vector matching.

It should also be pointed out that for larger search models this rotation function does not work as well as the conventional rotation function. Using the whole myoglobin structure as the search model in a global search, the signals for the correct solutions were not very strong. This is because matching too many 'vector' atoms in the model image can introduce too much noise that cannot be easily averaged out. Also, the number of translation peaks found for averaging for larger models is usually lower than that for smaller models. Therefore, our rotation function is more suitable for smaller search models, which could sometimes complement traditional rotation functions.

One of the main purposes of our method is to develop new methods for *ab initio* phasing using molecular replacement. Therefore, it is important to be able to limit the number of candidate peaks found in a global rotation search using a standard search model so that the subsequent translation search requires less computation. Our results show that the new rotation function has this potential.

The sponsor for this work was the National Natural Science Foundation of China (grant No. 10674172). The author thanks the reviewers for their critical and helpful comments on the paper.

References

Bentley, G. A. (1997). *Methods Enzymol.* **276**, 611–619.
Blow, D. M. (2006). *International Tables for Crystallography*, Vol. F, 1st online ed., ch. 13.1, pp. 263–268. Chester: International Union of Crystallography. [doi:10.1107/97809553602060000681]
Bricogne, G. (1997). *Methods Enzymol.* **276**, 361–423.
Brünger, A. T. (1997). *Methods Enzymol.* **276**, 558–580.
Brünger, A. T., Kuriyan, J. & Karplus, M. (1987). *Science*, **235**, 458–460.
Buerger, M. J. (1959). *Vector Space and Its Application in Crystal Structure Investigation.* New York: John Wiley & Sons.
Carter, C. W. Jr & Sweet, R. M. (1997). Editors. *Methods In Enzymology*, Vol. 276, pp. 558–619. New York: Academic Press.

Chang, G. & Lewis, M. (1997). *Acta Cryst.* D**53**, 279–289.
Chen, R., Li, L. & Weng, Z. P. (2003). *Proteins*, **52**, 80–87.
Collaborative Computational Project, Number 4 (1994). *Acta Cryst.* D**50**, 760–763.
Colman, P. M. & Fehlhammer, H. (1976). *J. Mol. Biol.* **100**, 278–282.
Dodson, E. J., Glover, S. & Wolf, W. (1992). Editors. *Proceedings of the CCP4 Study Weekend. Molecular Replacement.* Warrington: Daresbury Laboratory.
Glykos, N. M. & Kokkinidis, M. (2000). *Acta Cryst.* D**56**, 169–174.
Hoppe, W. & Paulus, E. F. (1967). *Acta Cryst.* **23**, 339–342.
Huber, R. (1965). *Acta Cryst.* **19**, 353–356.
Jiang, F. & Kim, S.-H. (1991). *J. Mol. Biol.* **219**, 79–102.
Jiang, F. & Rao, Z. (2001). *J. Synchrotron Rad.* **8**, 1051–1053.
Katchalski-Katzir, E., Shariv, I., Eisenstein, M., Friesem, A. A., Aflalo, C. & Vasker, I. A. (1992). *Proc. Natl Acad. Sci. USA*, **89**, 2195–2199.
Kissinger, C. R., Gehlhaar, D. K. & Fogel, D. B. (1999). *Acta Cryst.* D**55**, 484–491.
Lattman, E. E. (1972). *Acta Cryst.* B**28**, 1065–1068.
Liu, Q., Weaver, A. J., Xiang, T., Thiel, D. J. & Hao, Q. (2003). *Acta Cryst.* D**59**, 1016–1019.
Machin, P. A. (1985). Editor. *Proceedings of the CCP4 Study Weekend. Molecular Replacement.* Warrington: Daresbury Laboratory.
Morris, R. J., Perrakis, A. & Lamzin, V. S. (2002). *Acta Cryst.* D**58**, 968–975.
Navaza, J. (1987). *Acta Cryst.* A**43**, 645–653.
Nordman, C. E. (1966). *Trans. Am. Crystallogr. Assoc.* **2**, 29–38.
Nordman, C. E. (1972). *Acta Cryst.* A**28**, 134–143.
Nordman, C. E. (1994). *Acta Cryst.* A**50**, 68–72.
Nordman, C. E. & Nakatsu, K. (1963). *J. Am. Chem. Soc.* **85**, 353–354.
Read, R. J. (2001). *Acta Cryst.* D**57**, 1373–1382.
Read, R. J. (2006). *International Tables for Crystallography*, Vol. F, 1st online ed., ch. 15.2, pp. 325–331. Chester: International Union of Crystallography. [doi:10.1107/97809553602060000688]
Rossmann, M. G. & Blow, D. M. (1962). *Acta Cryst.* **15**, 24–31.
Schilling, J. W. (1970). *Crystallographic Computing*, edited by F. R. Ahmed, p. 115. Copenhagen: Munksgaard.
Storoni, L. C., McCoy, A. J. & Read, R. J. (2004). *Acta Cryst.* D**60**, 432–438.
Terwilliger, T. C. (2000). *Acta Cryst.* D**56**, 965–972.
Vagin, A. & Teplyakov, A. (1997). *J. Appl. Cryst.* **30**, 1022–1025.
Vagin, A. & Teplyakov, A. (2000). *Acta Cryst.* D**56**, 1622–1624.
Zhang, K. Y. J., Cowtan, K. D. & Main, P. (2006). *International Tables for Crystallography*, Vol. F, 1st online ed., ch. 15.1, pp. 311–324. Chester: International Union of Crystallography. [doi:10.1107/97809553602060000687]